

A search for $(\text{H}_2\text{O})_2$ in the Galaxy and toward comet Hale-Bopp

M. Scherer¹, M. Havenith¹, R. Mauersberger², and T.L. Wilson^{3,4}

¹ Institut für Angewandte Physik der Universität Bonn, Wegelerstr. 8, D-53115 Bonn, Germany

² Steward Observatory, The University of Arizona, Tucson, AZ 85721, USA

³ Max-Planck-Institut für Radioastronomie, Auf dem Hügel 69, D-53121 Bonn, Germany

⁴ Submillimeter Telescope Observatory, The University of Arizona, Tucson, AZ 85721, USA

Received 3 February 1998 / Accepted 21 April 1998

Abstract. The MPIfR 100 m telescope, the NRAO 12 m telescope, and the IRAM 30 m telescope were used to search for low lying rotational transitions of the water dimer, $(\text{H}_2\text{O})_2$, toward the Galactic cloud cores Orion-KL, W51 d, W51e1e2, NGC 7538, Sgr B2(M) and L134N, and toward comet Hale-Bopp. The comet was observed on December 20, 1996 and March 25/26, 1997 (i.e. near perihelion on April 1) at 24 GHz. No lines of $(\text{H}_2\text{O})_2$ were found. Our limit for the abundance of $(\text{H}_2\text{O})_2$ relative to that of water (from H_2^{18}O data) is typically $< 10^{-4}$ toward dense cloud cores. Toward Orion-KL an even more stringent limit of $< 8 \cdot 10^{-6}$ is derived. The abundance of $(\text{H}_2\text{O})_2$ relative to H_2 is typically $< 10^{-10}$. Our data show that at perihelion the production rate of the water dimer of comet C/1995 O1 (Hale-Bopp) was $< 5.7 \cdot 10^{29} \text{ s}^{-1}$. This is less than 6% the production rate of H_2O .

Key words: ISM: abundances – ISM: molecules – radio lines: ISM – line: identification – molecular processes – comets: individual: C/1995 O1 (Hale-Bopp)

1. Introduction

Between any molecules one can find a weak attractive interaction. This so called van der Waals interaction is due to electrostatic forces, induction and dispersion, the first two depending strongly on the relative position of the partners. If this attraction is stronger than the repulsion between the two molecules, stable complexes, which are also known as “dimers”, can form. These bonds are usually weak compared to chemical bonds.

Emission from dimers has been detected in planetary atmospheres (Frommhold et al. 1984). It is unknown how much of the mass of the interstellar medium (ISM) is tied up in such dimers. It has even been suggested that some of the dark matter in the outer part of disk galaxies may consist of H_2 dimers (see the discussion in Combes & Pfenniger 1997). Dimers have been proposed to be a major constituent of cometary matter (Krasnopolsky et al. 1988). Interstellar grain mantles, which are thought to be similar in composition to cometary ices may be a reservoir for dimers.

Send offprint requests to: M. Havenith

The few previous searches (e.g. Liszt 1978, Vanden Bout et al. 1979, CO-CO; Schenewerk et al. 1985, HCN-HCN) were unsuccessful, partly because no reliable laboratory measurements were available. Within the last years there has been significant progress in this field. New experimental techniques were developed which give access to precise transition frequencies.

After H_2 , the next most abundant molecule is believed to be CO, which has a dipole moment of only 0.1 Debye. The H_2 -CO dimer is only weakly bound. Although the large abundances of CO and H_2 may be favorable for the production of H_2 -CO, the bond of this complex is easily destroyed by shock waves. The limits recently obtained for this dimer (Allen et al. 1997) show that this complex is not very abundant in the ISM.

We have searched for the $(\text{H}_2\text{O})_2$ complex toward Galactic sources and toward comet C/1995 O1 (Hale-Bopp). The dimer is composed of two rare molecules, and therefore requires very high densities to be produced in the gas phase. Our decision to search for $(\text{H}_2\text{O})_2$ was based on four reasons: First, the transition frequencies are well known. Second, water is rather abundant in ices in interstellar cores and cometary nuclei. Therefore dimers have a chance to form. Third, from the observations of deuterated water, grain mantle evaporation is a common phenomenon in hot molecular cores (Gensheimer et al. 1996). Finally, the relatively strong bond suggests that water dimer might survive the evaporation process and has a comparably long lifetime in the interstellar and interplanetary gas.

2. The water dimer

2.1. The structure of $(\text{H}_2\text{O})_2$

The water dimer is a simple type of a hydrogen bonded complex. The binding energy of this kind of intermolecular bond is between the pure van der Waals bonds, which are typically in the range of 10–20 meV and chemical bonds (e.g. CO: 11.2 eV). The binding energy for $(\text{H}_2\text{O})_2$ is 0.22 eV (2500 K), and it corresponds to half the binding energy of the weakest chemical bond (i.e. that of the Cs_2 molecule). The structure of the water dimer has been deduced from measurements by Dyke et al. (1977) and Odutola et al. (1988). The structural information was obtained from microwave and radiofrequency measurements using isotopic substitution effects, Stark effect measurements and mea-

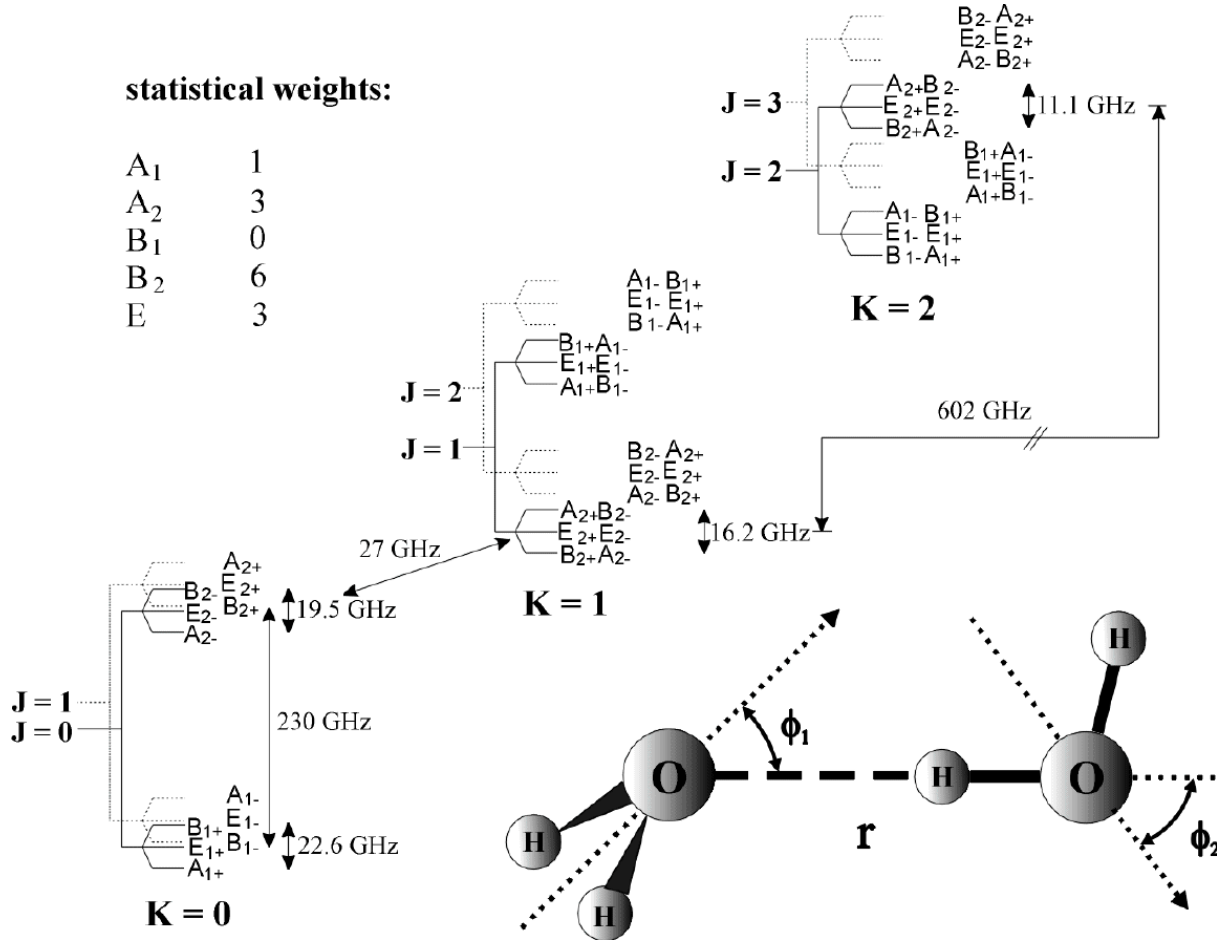


Fig. 1. The structure of the water dimer, and its energy level diagram. The (J, K) asymmetric top levels are shown for each of the six tunneling states (A_{1,2}, B_{1,2}, E_{1,2}). For the $K = 1$ and $K = 2$ levels, the asymmetry doubling is neglected.

Table 1. Observed (H₂O)₂ lines

$J', K', \Gamma' - J'', K'', \Gamma''$	ν GHz.	ΔE^b K	μ_{ij}^2 D ²	$f(5\text{ K})^a$ 10 ⁻³	$f(10\text{ K})^a$ 10 ⁻³	$f(100\text{ K})^a$ 10 ⁻³
2,0E ⁻ — 1,0E ⁺	24.28432	10.2	4.6	14.5	5.2	0.16
6,0E ⁺ — 5,0E ⁻	73.88403	9.4	3.8	17.1	20.7	0.60
8,0A ₂ ⁻ — 7,0A ₂ ⁺	78.75559	26.6	3.7	0.54	5.0	0.68
7,0E ⁻ — 6,0E ⁺	86.17950	12.9	3.7	8.4	17.2	0.68
6,1B ₂ ⁻ — 5,1B ₂ ⁺	91.08690	20.8	3.7	3.4	13.2	1.1
9,0B ₂ ⁺ — 8,0B ₂ ⁻	91.09928	31.3	3.7	0.42	7.1	1.5
6,0B ₂ ⁻ — 5,0B ₂ ⁺	92.33456	17.9	3.8	6.1	17.6	1.1

a) fraction of molecules which are in the lower state, see Sect. 2.3

b) energy of the lower level above the ground state

measurements of the hyperfine structure. The resultant structure, which is shown in Fig. 1 together with an energy level diagram, has an oxygen-oxygen distance, r , of 2.98 Å. The proton accepting and donating water axes have an angle of $\phi_1 = 58(6)$ and $\phi_2 = 51(6)$ degrees with respect to the intermolecular axis connecting the two oxygen molecules and the proton donating axis, respectively. The structure deduced from the measurements is in excellent agreement with that predicted by ab initio calculations (Matsuoka et al. 1976, Odutola et al. 1988, Amos 1986).

This structure is consistent with a linear hydrogen bond and the proton acceptor tetrahedrally oriented to the hydrogen bond. Stark effect measurements on different rotational lines yielded the dipole moment of (H₂O)₂ (Dyke 1977). A least-squares fit of the second order Stark coefficient C_2 led to $\mu_a = 2.633(4)$ D and $\mu_b \cong \mu_c \cong 0$ D (Coudert et al. 1987), which is in good agreement with that determined by Dyke et al. (1977).

2.2. Tunneling modes and level pattern of (H₂O)₂

Although one might think of the water dimer as a molecule which has a definite structure, e.g. binding length and angles, the spectrum is greatly complicated by the effect of tunneling motions of the constituent H₂O molecules. The observed spectrum could only be interpreted in terms of a theoretical model which includes all feasible proton-exchange tunneling motions in the dimer (Dyke et al. 1977). It is assumed that all tunneling splittings are small compared to the vibrational frequencies of the dimer. As a consequence each rotational level of the C_s symmetry of the water dimer is split into six sublevels (Fig. 1). Each of these six vibrational tunneling levels has its own statistical weight and rotational structure, and only a small number of them are following a near rigid-rotor type pattern.

It was possible to fit all measured data using a model as developed by Hougen (1985), Coudert et al. (1987) and Coudert & Hougen (1988, 1990), which shows the existence of four large amplitude motions. The tunneling with the lowest barrier corresponds to a 180° rotation of the hydrogen accepting H₂O monomer about its two-fold axis of symmetry during which the hydrogen bond in the axis is not changed. This motion leads to a splitting into two states, separated by approximately 200 GHz. The next most likely motion is an interconversion tunneling motion, in which the hydrogen donor/acceptor roles of the two water monomers are interchanged. Formally, this motion corresponds to a 90° geared rotation of each monomer about its two-fold axis of symmetry, accompanied by simultaneous readjustment of the wagging angles. This motion splits each of the levels into three states, one of them being doubly degenerate. The magnitude of the splitting between the upper and lower level in the pattern amounts to 19 GHz. The other two tunneling motions are the following: A geared rotation of both monomers about axes perpendicular to the plane of symmetry of the dimer by which the hydrogen in the hydrogen bond is changed and a 90° anti-g geared rotation of the two monomer units about their two-fold axis of symmetry accompanied by wagging readjustments. These further tunneling motions had to be proposed as a consequence of measurements (Hougen 1985).

The high resolution data set (see Coudert et al. 1987 for an overview) include microwave measurements as obtained by Dyke (1977), Coudert et al. (1987), Martinache et al. (1988), and Fraser et al. (1989 a, b) as well as FIR data of Busarow et al. (1989). We searched for water dimer lines in the interstellar medium at transitions around 24 and 74–92 GHz as listed in Coudert & Hougen (1990).

2.3. The partition function

Since only a small number of transitions have been measured so far, most of the levels had to be predicted to obtain the partition function. This is given by $p(T_{\text{ex}}) = \sum g_i (2J_i + 1) \exp(-E_i/kT_{\text{ex}})$ (g_i statistical weight, see Fig. 1, E : energy above the ground, T_{ex} : excitation temperature). We followed the model developed in Dyke (1977) and Coudert & Hougen (1988, 1990) neglecting the K asymmetry doubling. This cor-

responds to an extrapolation of the measured energy pattern toward higher energies. In addition, we considered all low lying van der Waals modes of (H₂O)₂. These are expected to be at 125 cm⁻¹, 142 cm⁻¹, 149 cm⁻¹, 174.5 cm⁻¹, 365.5 cm⁻¹ and 597 cm⁻¹ following the calculation of Amos (1986). In Table 1, we list $f(T_{\text{ex}})$, the fraction of all water dimer molecules which are in the lower state of the observed transition for typical values of T_{ex} . At high excitation, many levels are populated. This tends to decrease f for a given state. The 3 mm transitions chosen for our search are typically 20 or 30 K above the ground state. Therefore they are quite well matched to be observed toward hot cores. We chose not to search for lines with a higher J because their frequencies are less well determined and because excitation conditions are less clear.

2.4. Dipole matrix elements

The dipole matrix elements $\mu_{ij}^2 = \mu^2 S / (2J_l + 1)$ are required to estimate the column density from the observed line intensities (see Eq. 1). J_l is the rotational quantum number of the lower level involved and μ is the dipole moment. We assumed $\mu \sim \mu_a \sim 2.6$ D. S is the line strength, which is tabulated in the Appendix V of Townes & Schawlow (1975).

Since (H₂O)₂ is far from being a rigid asymmetric top molecule, the rotational constants A , B , and C lose their meaning as structural parameters. The E -type symmetry is the symmetry which follows most closely a rigid rotor type pattern. We have therefore fitted A , B and C values for E -type transitions and have calculated μ_{ij} for all symmetries using these constants. However, these values are only rough estimates since for transitions of the A and B symmetries, a tunneling motion is involved. For a rigorous calculation of the line strength, the tunneling path would have also to be taken into account. Since (H₂O)₂ is close to being a prolate molecule, we assumed that the value κ (see Townes & Schawlow 1975) is about -1 . Therefore, the quantum number K in our nomenclature equals approximately K_{-1} in Townes & Schawlow (1975). The derived estimates for μ_{ij}^2 based on this structure are given in Table 1.

3. Observations

The transitions which we observed were taken from the list of Coudert & Hougen (1990). These are listed in Table 1 together with their quantum numbers and their tunneling state Γ .

The observations have been made using the NRAO 12 m telescope¹ on Kitt Peak (beam width $\sim 60''$ at the search frequencies), the IRAM 30 m telescope on Pico Veleta (beam: 30''), and the MPIfR 100 m telescope in Effelsberg (beam: 38''). For all measurements we employed the position switching mode. The focus and pointing corrections were based on continuum scans through nearby continuum sources. The 100 m data were calibrated using continuum measurements of 3C 48, assuming a flux density of 1.1 Jy (Ott et al. 1994). The data observed with

¹ The National Radio Astronomy Observatory is a facility of the National Science Foundation operated under cooperative agreement by Associated Universities Inc.

Table 2. H₂O Dimer line search results

Source ^a	Telesc.	ν GHz.	Date dd/mm/yy	RMS ^b mK	N_l^g 10^{10} cm^{-2}	N_{tot}^h 10^{13} cm^{-2}
Ori-KL	100 m	24.284	22/12/96	3 ^c	<10	<63
	100 m	24.284	26/3/97	4	<13	<81
	12 m	78.756	3/6+22/996	6	<8	<12
	12 m	86.180	2/6 +22/9/96	20 ^f	<23	<34
	30 m	86.180	27/8/96	20 ^f	<23	<34
	12 m	91.087	2/6/96	6	<7	<7
	30 m	91.087	26/8/96	20 ^e	<22	<21
	12 m	91.099	2/6/96	6	<7	<5
	30 m	91.099	26/8/96	7	<8	<5
	30 m	92.335	25-26/8/96	9 ^d	<9	<8
L134N	12 m	86.179	2/6/96	6	<2.5	<0.3
SgrB2(M)	100 m	24.284	20/12/96	18	<89	<560
W51d	100 m	24.284	21/12/96	3	<15	<94
	12 m	73.884	30/6+22/9/96	10	<20	<33
	12 m	78.756	3-4/6/96	6	<11	<16
	12 m	86.180	2/6/96	3 ^f	<5	<7
	30 m	86.180	25-31/8/96	10 ^f	<17	<25
	12 m	91.087	4/6+22/9/96	3	<5	<5
	30 m	91.087	24-27/8/96	9	<15	<14
	12 m	91.099	4/6+22/9/96	3	<5	<3
	30 m	91.099	24-27/8/96	9	<15	<10
	30 m	92.335	24/8/96	12	<19	<17
W51e1/e2	30 m	86.180	25/8/96	20 ^f	<42	<62
	30 m	91.087	24/8/97	15	<30	<28
	30 m	91.099	24/8/97	15	<30	<20
	30 m	92.335	24/8/97	11	<21	<19
NGC7538	12 m	86.180	2/6/96	4 ^f	<5	<7
Hale-Bopp	100 m	24.284	21/12/96	9 ^c	<7	<44
	100 m	24.284	25-26/3/97	10 ^c	<8	<50

a) Source positions (α_{1950} , δ_{1950}) and assumed LSR velocities are: Orion KL: $5^{\text{h}}32^{\text{m}}46^{\text{s}}.7$, $-05^{\circ}24'24''$, 8.0 km s^{-1} ; L134N: $15^{\text{h}}51^{\text{m}}32^{\text{s}}.7$, $-02^{\circ}42'51''$, 2.5 km s^{-1} ; Sgr B2(M): $17^{\text{h}}44^{\text{m}}10^{\text{s}}.6$, $-28^{\circ}22'00''$, 60.0 km s^{-1} ; W51d: $19^{\text{h}}21^{\text{m}}22^{\text{s}}.0$, $+14^{\circ}25'17''$, 60.0 km s^{-1} ; W51e1e2: $19^{\text{h}}21^{\text{m}}26^{\text{s}}.3$, $+14^{\circ}24'36''$, 60.0 km s^{-1} ; NGC 7538: $23^{\text{h}}11^{\text{m}}36^{\text{s}}.5$, $+61^{\circ}11'49''$, -56.5 km s^{-1}

b) The RMS refer to a channel width of 3.6 km s^{-1} , except for L134 and Hale-Bopp, where they refer to 1.2 km s^{-1} wide channels.

c) In Orion, the $2_{02} - 1_{01}\text{E}$ and $2_{02} - 1_{01}\text{A}$ lines of CH₃OHCO (methyl formate, rest frequencies 24.29652 and 24.29847, Lovas 1991) were observed in the same band with an intensity of 113 and 133 mK. The rest velocity is 7.9 km s^{-1} and the line width 2.3 km s^{-1} . These lines were not detected toward comet Hale-Bopp.

d) this limit is determined by line confusion

e) this limit is estimated taking into account a blend with a line at 91.0896 GHz (assuming $v_{\text{LSR}}=6 \text{ km s}^{-1}$). A Gaussian fit to that line yields $T_{\text{MB}}=78 \text{ mK}$ and $\Delta v_{1/2} = 10(1) \text{ km s}^{-1}$.

f) this limit is taking into account a blend with the $6_7 - 5_6$ line of CCS (rest frequency: 86.1814 GHz, Lovas 1991). A Gaussian fit of the 30 m data to the CCS line in Orion yields $T_{\text{MB}} = 54 \text{ mK}$ and $\Delta v_{1/2} = 3.4 \text{ km s}^{-1}$, and toward W51d: $T_{\text{MB}} = 31 \text{ mK}$ and $\Delta v_{1/2} = 12 \text{ km s}^{-1}$, W51e1/e2: $T_{\text{MB}} = 87 \text{ mK}$ and $\Delta v_{1/2} = 7 \text{ km s}^{-1}$. From the 12 m data for NGC 7538, the CCS line has $T_{\text{MB}} = 20 \text{ mK}$ and $\Delta v_{1/2} = 4 \text{ km s}^{-1}$

g) N_l was estimated using 3 times the RMS and the linewidth expected for thermal water lines: 7.3 km s^{-1} for Ori-KL, 11 km s^{-1} for Sgr B2(M) and W51d, 13.5 km s^{-1} for W51e1e2, 8.5 km s^{-1} for NGC 7538 (Gensheimer et al. 1996), 1.8 km s^{-1} for Hale-Bopp (e.g. Bird et al. 1997), and 1.1 km s^{-1} for L134N (Swade & Schloerb 1992).

h) Computed from N_l and a partition function based on a common T_{ex} of 5 K for L134N and 100 K for all other sources.

the 30 m and 12 m telescopes were calibrated using a chopper wheel method. All temperatures are given on a main-beam brightness temperature scale.

At the MPIfR 100 m telescope, a K-band maser was used. The system noise corrected for absorption in the earth's atmosphere and telescope efficiency is $\sim 300 \text{ K}$. The spectrometer was a 1024 channel autocorrelator with a channel separation of 50 or 100 kHz, corresponding to a velocity resolution of 0.6 or

1.2 km s^{-1} . For the perihelion observations of Hale-Bopp, we used the same ephemeris and observing procedures as described in Bird et al. (1997).

At the NRAO 12 m telescope, a dual channel, single side-band, SIS receiver with typical system temperatures of 250 K was used. As spectrometers we placed either half of a 1024 channel hybrid spectrometer on each of the two receiver channels. The channel separation was 97 kHz (i.e. $\sim 1.2 \text{ km s}^{-1}$).

Only for the dark cloud L134N, we used a higher resolution of 24 kHz (0.3 km s⁻¹).

At the IRAM 30 m telescope two single channel SIS receivers were used. As backends we used filterbanks with a channel separation of 1 MHz (3.6 km s⁻¹).

4. Results and discussion

The results of our search are summarized in Table 2. In all cases, only upper limits to the emission of the water dimer can be given.

4.1. The interstellar abundance of water dimers

We computed limits to the beam averaged column densities in the lower levels, N_l , of the observed transitions given in Table 2 using

$$N_l = \eta 1.67 \cdot 10^{14} \text{ cm}^{-2} \frac{\int T_{\text{MB}} dv}{\nu \mu_{ij}^2}, \quad (1)$$

with

$$\eta = \frac{T_{\text{ex}}}{T_0} \left(\frac{1}{\exp(T_0/T_{\text{ex}}) - 1} - \frac{1}{\exp(T_0/2.7 \text{ K}) - 1} \right)^{-1} \quad (2)$$

Here, $\int T_{\text{MB}} dv$ is the integrated line intensity in K km s⁻¹, $T_0 = h\nu/k$, ν is the line frequency in GHz and the dipole matrix element (see Sect. 2.4) $\mu_{ij}^2 = \mu^2 S/(2J_l + 1)$ is in D². This equation is valid for optically thin emission (see Rohlfs & Wilson 1996). The values of N_l given in Table 2 correspond to three times the measured RMS and to the expected line width in each source. Using the function $f(T_{\text{ex}})$ and the individual N_l given in Table 1, we estimate limits to the total column density, N_{tot} ; these are typically $5 \cdot 10^{13} \text{ cm}^{-2}$. We assumed $T_{\text{ex}} = 100 \text{ K}$ for Hale-Bopp (Bird et al. 1997) and also for the Galactic hot cores. Although the kinetic temperatures in these hot cores may in some cases exceed 200 K (Mauersberger et al. 1996), our beam probably also picks up emission from a more extended, cooler component. Only for the dark cloud L134N, we assumed a value of 5 K (Swade 1989). For each of the sources, we compile the most stringent limits obtained from the individual observations in Table 3. These are compared to the column densities of H₂O and H₂ obtained with beamsizes similar to that of our water dimer measurements. The abundance of (H₂O)₂ relative to that of water is typically $< 10^{-4}$ toward the dense cloud cores; toward Orion-KL an even more stringent limit of $8 \cdot 10^{-6}$ is derived. The abundance of (H₂O)₂ relative to H₂ is typically $< 10^{-10}$.

It is interesting that the 91.087 GHz line frequency used in our search happens to be in the spectrometer band used by Allen et al. (1997) to search for CO-H₂. In none of their sources (TMC 1, L 1157, 2013+370 and L 134 at a position different than ours) did they detect a signal. The typical noise they quota for a 1 MHz channel was 5 mK for the dark clouds. This is similar to the limit we report for L134N, although our velocity resolution is much finer to search for narrow lines, which are characteristic for such cold clouds, and we conclude that the column densities of (H₂O)₂ are $\lesssim 10^{12} \text{ cm}^{-2}$, as in L 134N.

We summarize that water dimers apparently make up only a small fraction of the water in the dense interstellar medium, even in hot cores where complex molecules have recently evaporated from grains and where chemical equilibrium still has not been reached. It is not clear whether this is due to a lack of such complexes in evaporating interstellar ice, whether the bonds are destroyed in the process of evaporation or whether the chemical timescales in which water dimers react and recondense into larger clusters are just too short.

4.2. Water dimers toward comet Hale-Bopp

Molecules are destroyed by the solar UV field within typically several 1000 s after they have evaporated from the surface of a comet. Murad & Bochsler (1987) estimated that the lifetime of the water dimer in the solar radiation field is 10^4 s at a distance of 1 AU, which is an order of magnitude smaller than the lifetime of water.

For an unresolved source, the molecular production rate Q is related to the beam averaged column density N by

$$Q(\text{mol}) = N(\text{mol}) \frac{\pi \Delta^2 \theta^2}{4\tau r_{\text{AU}}^2} \quad (3)$$

(Snyder 1982). Here, Δ is the geocentric distance (in cm), r_{AU} is the heliocentric distance of the comet in AU, θ is the beam width of the telescope in radian. This can be written in more convenient units:

$$Q(\text{mol}) = 4.1 \cdot 10^{15} N(\text{mol}) \frac{(\theta'')^2 \Delta_{\text{AU}}^2}{\tau r_{\text{AU}}^2}, \quad (4)$$

where θ'' is the beamwidth in arcseconds, Q is in s⁻¹ and N in cm⁻². From our March 1997 observation, the upper limit of the production rate of the water dimer in Comet Hale-Bopp was $5.7 \cdot 10^{29} \text{ s}^{-1}$ (with $\tau = 10^4 \text{ s}$, $\Delta = 1.35 \text{ AU}$, $r = 0.97 \text{ AU}$, $\theta = 38''$). The water production rate at that time is still debated. Schleicher et al. (1997) and Dello Russo et al. (1997) estimate a value of $4\text{--}5 \cdot 10^{30} \text{ s}^{-1}$, while a value of $1 \cdot 10^{31} \text{ s}^{-1}$ has been proposed from radio observations of OH (Colom et al. 1998). Assuming that the radio data give a more reliable estimate of $Q(\text{H}_2\text{O})$, an upper limit for the relative production rate of the water dimer is therefore $< 6\%$.

This does not necessarily reflect the conditions at the cometary surface, since (H₂O)₂ can be chemically produced and destroyed in the coma after the evaporation process, and water dimers will partly recondense into large clusters as pointed out by Crifo & Slanina (1991). Our limit casts doubt on the suggestion by Krasnopolsky et al. (1988) that water dimers make up 25% of cometary parent molecules; it is consistent with the models by Crifo & Slanina (1991), which predict an abundance of 10^{-5} .

Note that for excitation temperatures around 100 K the lines in the 3 mm range are much more sensitive indicators of the column density of water dimers than the 24 GHz line we observed. Unfortunately we had not been granted time at a mm-wave telescope around Hale-Bopp's perihelion. It is, however,

Table 3. 3 σ limits of column densities and relative abundances of (H₂O)₂

Source	beam "	$N((\text{H}_2\text{O})_2)^a$ 10^{13} cm^{-2}	$N(\text{H}_2\text{O})$ 10^{17} cm^{-2}	$N(\text{H}_2)$ 10^{23} cm^{-2}	$\frac{(\text{H}_2\text{O})_2}{\text{H}_2\text{O}}$ 10^{-4}	$\frac{(\text{H}_2\text{O})_2}{\text{H}_2}$ 10^{-10}	Ref. ^b
Ori-KL	30	<5	61	10	<0.08	<0.5	1,2
L134N	60	<0.3	-	0.065	-	<4.6	3
SgrB2(M)	36	<560	-	22	-	<25	4
W51d	30	<10 ^d	4.3	5	<2.3	<2.0	1, 5
W51e1/e2	30	<19	7.9	10	<2.4	<1.9	1, 5
NGC 7538	60	<7	0.35 ^c	0.6	<20	<12	6, 7
Hale-Bopp	38	<50 ^e	-	-	<600	-	8

a) 3 σ limits

b) Refs.: 1: Jacq et al. (1990), 2: Keene et al. (1982), 3: Swade (1989), 4: Goldsmith et al. (1987), 5: Jaffe et al. (1984), 6: Gensheimer et al. (1996), 7: Werner et al. (1979), 8: Colom et al. 1998

c) Scaling the 12'' data to a 1' beam assuming an unresolved H₂O source.

d) the most stringent limit for a 30'' beam

e) at perihelion

worthwhile to investigate other line observations for a serendipitous detection of one of the numerous mm-wave transitions of (H₂O)₂. For this, we suggest to use the compilation of transition frequencies by Coudert & Hougen (1990). Even a non-detection could yield much lower limits for the relative abundance of the water dimer than we were able to obtain.

We detected the 2₀₂ – 1₀₁E and 2₀₂ – 1₀₁A lines of CH₃OHCO (methyl formate) toward Orion-KL but not toward comet Hale-Bopp. From this non-detection, the limit to the production rate of this molecule is consistent with the production rate estimated from a mm-wave detection of CH₃OHCO by Colom et al. (1997).

5. Conclusions

We have searched for several lines of the water dimer, (H₂O)₂, toward Galactic hot cores and for one line toward one Galactic dark cloud and toward comet Hale-Bopp. Our main conclusions are:

- No emission of water dimer lines was detected. This leads to upper limits of the (H₂O)₂/H₂O abundance of typically 10⁻⁴ and in the case of Orion of 8 10⁻⁶. Together with the limits for the CO-H₂ given by Allen et al. (1997) these are the most stringent limits given for van der Waals complexes in the ISM.
- Our nondetection of the water dimer toward comet Hale-Bopp limits the production rate to < 5.7 10²⁹ s⁻¹ at perihelion, and the (H₂O)₂/H₂O abundance to < 6%. We suggest to look for serendipitous detections of (H₂O)₂ in archived observations of Hale-Bopp.

Acknowledgements. We thank Dr. P. Gensheimer who assisted in the measurements at the 30 m telescope. We thank the referee, Dr. J. Crovisier, for valuable comments. This work was supported by a Bennigsen-Foerder Research Prize granted to M.H. by the Land Nordrhein Westfalen. R.M. was supported by a Heisenberg fellowship by the Deutsche Forschungsgemeinschaft.

References

- Allen R.J., Loinard L., McKellar A.R.W., Lequeux J., 1997, ApJ 489, 102
- Amos R.D., 1986, Chem. Phys. 104, 145
- Bird M.K., Huchtmeier W.K., Gensheimer P. et al., 1997, A&A 325, L5
- Busarow K.L., Cohen R.C., Blake G.A. et al., 1989, J. Chem. Phys. 90, 3937
- Colom P., Despois D., Germain B., et al., 1997, IAU Circ. 6645
- Colom P., Gérard E., Crovisier, J., et al., 1998, in: First International Conference on Comet Hale-Bopp, Tenerife, Spain, in press
- Combes F., Pfenniger D., 1997, A&A 327, 453
- Coudert L.H., Hougen J.T., 1988, J. Mol. Spectrosc. 130, 86
- Coudert L.H., Hougen J.T., 1990, J. Mol. Spectrosc. 139, 259
- Coudert L.H., Lovas F.J., Suenram R.D., Hougen J.T., 1987, J. Chem. Phys. 87, 6290
- Crifo J.F., Slanina Z., 1991, ApJ 383, 351
- Dello Russo N., Mumma M.J., DiSanti M.A., et al., 1997, IAU Circ. 6682
- Dyke T.R., 1977, J. Chem. Phys. 66, 492
- Dyke T.R., Mac, K.M., Muentner J.S., 1977 J. Chem. Phys. 66, 498
- Fraser G.T., Suenram R.D., Coudert L.H., 1989a, J. Chem. Phys. 90, 6077
- Fraser G.T., Suenram R.D., Coudert L.H., Frye R.S., 1989b, J. Mol. Spectrosc. 137, 244
- Frommhold L., Samuelson R., Birnbaum G., 1984, ApJ 283, L79
- Gensheimer P.D., Mauersberger R., Wilson T.L., 1996, A&A 314, 281
- Goldsmith P.F., Snell R.L., Lis D.C., 1987, ApJ 313, L5
- Hougen J.T., 1985, J. Mol. Spectrosc. 114, 395
- Jacq T., Walmsley C.M., Henkel C. et al. 1990, A&A 228, 447
- Jaffe D.T., Becklin E.E., Hildebrand R.H., 1984, ApJ 279, L51
- Keene J., Hildebrand R.H., Whitcomb S.E., 1982, ApJ 252, L11
- Krasnopolsky V.A., Tkachuk A. Yu., Moreels G., Gogoshev M., 1988, A&A 203, 175
- Liszt H.S., 1978, ApJ 219, 454
- Lovas F.J., 1991, J. Phys. Chem. Ref. Data 21, 181
- Martinache L., Jans-Burli S., Vogelsanger B., Kresa W., Bauder A., 1988, Chem. Phys. Lett. 149, 424
- Matsuoka O., Clementi E., Yoshimine M., 1976, J. Chem. Phys. 64, 1351
- Mauersberger R., Henkel C., Wilson T.L., Walmsley C.M., 1986, A&A 162, 199

- Murad E., Bochsler P., 1987, *Nat* 326, 366
- Odutola J.A., Hu T.A., Prinslow D., O'dell S.E., Dyke T.R., 1988, *J. Chem. Phys.* 88, 5352
- Ott M., Witzel A., Quirrenbach A., et al., 1994, *A&A* 284, 331
- Rohlfs K., Wilson T.L., 1996, *Tools of Radioastronomy*, Springer Verlag
- Schenewerk M.S., Jewell P.R., Snyder L.E. et al., 1985, *ApJ* 296, 218
- Schleicher D.G., Millis R.L., Farnham T.L., Lederer S.M., 1997, *BAAS* 29, 32.04
- Snyder L.E., 1982, *Icarus* 51, 1
- Swade D.A., 1989, *ApJ* 345, 828
- Swade D.A., Schloerb P.F., 1992, *ApJ* 392, 543
- Townes C.H., Schawlow A.L., 1975, *Microwave Spectroscopy*, Dover
- Vanden Bout P.A., Steed J.M., Bernstein L.S., Klemperer W., 1979, *ApJ* 234, 503
- Werner M.W., Becklin E.E., Gatle I. et al., 1979, *MNRAS* 188, 463